Lake surface water temperature [in "State of the Climate 2020"]

Article

Published Version

over the Great Lakes are adjusted as described in Simmons et al. (2021) to correct for a production error. This correction has a negligible impact on the global average temperature. The other reanalysis, JRA-55, provides data from 1958 onward. The JRA-55 global average temperature is computed as in Simmons et al. (2017, 2021), that is by using JRA-55 analysis temperature over land and its background temperature over ocean and other water bodies. For both reanalyses, the 2-m air temperature is used over both land and ocean whereas the global in situ analyses use SST over ocean. This difference is expected to have only a very small impact on the global averages assessed here (see Fig. 1 of Simmons et al. 2017).

While annual temperature rankings provide an intuitive measure of the state of global temperatures, a recently introduced global annual temperature score (Arguez et al. 2020) complements the annual temperature ranking by providing a basic characterization of the impacts of interannual variability on global temperature relative to the sustained upward trend since the mid-1970s. Scores range from 1 to 10, with a score of 1 (10) indicating the coldest (warmest) 10% of anomalies relative to the trend. In an era of seemingly perpetual near-record warm rankings, the annual temperature scores can help characterize whether the annual temperature ranking attained in a given year was due primarily to the secular trend, interannual variability, or both. For example, 2016 was not only the warmest year on record, but it also exhibited a temperature score of 10, whereas 2014 previously attained a ranking of warmest yet exhibited a temperature score of 4 (on the colder half of the scale). This indicates that, on top of the secular trend, interannual variability had a prominent contribution to the record temperature in 2016, whereas interannual variability did not synergistically contribute to 2014's previous record temperature. Using global annual time series from 1975 through 2020, the year 2020 registers a global annual temperature score of 9 (corresponding to the 80th–90th percentile) in the NASA-GISS and NOAAGlobalTemp datasets and a score of 8 (70th–80th percentile) in the HadCRUT5 dataset. This indicates that 2020, much like 2019, was moderately-to-considerably warmer than would be expected due to the secular trend alone, suggesting that its ranking of warmest or second warmest for the three in situ datasets was enhanced by the effects of the interannual variability.

Separately, the global land surface temperature for 2020 was the highest in four of the five datasets, surpassing the previous record set in 2016 by 0.05°–0.11°C. The fifth dataset (JRA-55) has the global land surface temperature tying with 2016 as the highest. The globally averaged SST was either third or fourth highest on record, depending on the dataset.

The year was characterized by higher-than-average temperatures across much of the globe (Plate 2.1a; Appendix Figs. A2.1–A2.4). The most notable feature of 2020 is the very large positive temperature anomalies (+4.0°C or higher above the 1981–2019 base period) over Arctic Siberia and the adjacent sector of the Arctic Ocean (Appendix Fig. A2.2). Large positive anomalies (+2.0°C or higher) are also found across northern Europe, northern Asia, and the North Pacific Ocean. In contrast, average to below-average conditions were limited to the central and eastern tropical Pacific Ocean and across parts of northern North America, subpolar North Atlantic, and the southern Indian Ocean.

2) Lake surface water temperature—L. Carrea, C. Merchant, B. Calmettes, and J.-F. Cretaux

In 2020, the worldwide averaged satellite-derived lake surface water temperature (LSWT) warm-season anomaly was +0.11°C with respect to the 1996–2016 baseline. The mean warming trend during 1996–2020 was 0.22 ± 0.01°C decade^{-1}, broadly consistent with previous analyses (Woolway et al. 2017; Woolway et al. 2018; Carrea et al. 2019, 2020). On average, anomalies in 2020 were only 0.01°C higher than in 2019. The warm-season anomalies for each lake are shown in Plate 2.1b. Lake mean temperature anomalies were positive for 55% of lakes and negative for 45%. Some lakes in eastern Africa recorded notable positive anomalies for both LSWT and lake water level (LWL; section 2d6). The LWL is defined as the height, in meters above the geoid (the shape that the surface would take under the influence of the gravity and rotation of Earth), of

the reflecting surface. Changes in lake water levels can be critical, as they affect water quantity and quality, food stocks, recreational opportunities, and transportation.

Globally, distinct regions of coherent warm and cool LSWT anomalies can be identified in 2020. Lakes in subtropical eastern China were markedly warm, with the three largest warm anomalies (+2.54°C, +2.39°C, +2.38°C) in this region. In northern Europe, Canada, the southeastern United States, and southeastern Australia, negative anomalies were observed for 70% or more of the water bodies, while southern Europe, Alaska, the Middle East, northern Russia, and eastern Africa had positive anomalies.

Four regions are considered here in more detail: Canada (number of lakes, n = 246, Fig. 2.2); Europe (n = 127, Fig. 2.2); Tibet (n = 104, Fig. 2.2); and Africa (n = 70). The boreal warm season (July–September) LSWT calculated from the satellite data shows a warming tendency of +0.39 ± 0.01°C decade^{-1} in Europe (Fig. 2.2a) and +0.18 ± 0.01 °C decade^{-1} in Canada (Fig. 2.2d). In Africa and Tibet, the tendency is closer to neutral (Figs. 2.2b,c). In Canada, 166 lakes had negative anomalies and 80 had positive in 2020, with an overall average of −0.22°C. In Tibet, 72% of the lakes had moderate-positive anomalies and 28% had negative anomalies, with an average of +0.20°C. In Europe, cool anomalies in northern Europe (67 lakes) balanced warmer anomalies in the south (60 lakes), producing +0.03°C on average. In Africa, positive anomalies were recorded for 80% of the 70 lakes over the considered period. Several of the warmest anomalies occurred in eastern Africa, where the LWL was also consistently higher than the 1996–2016 average. Therefore, for some of the eastern African lakes, LSWT was compared with their LWL anomalies, calculated using a time series of LWL changes obtained from satellite altimetry.

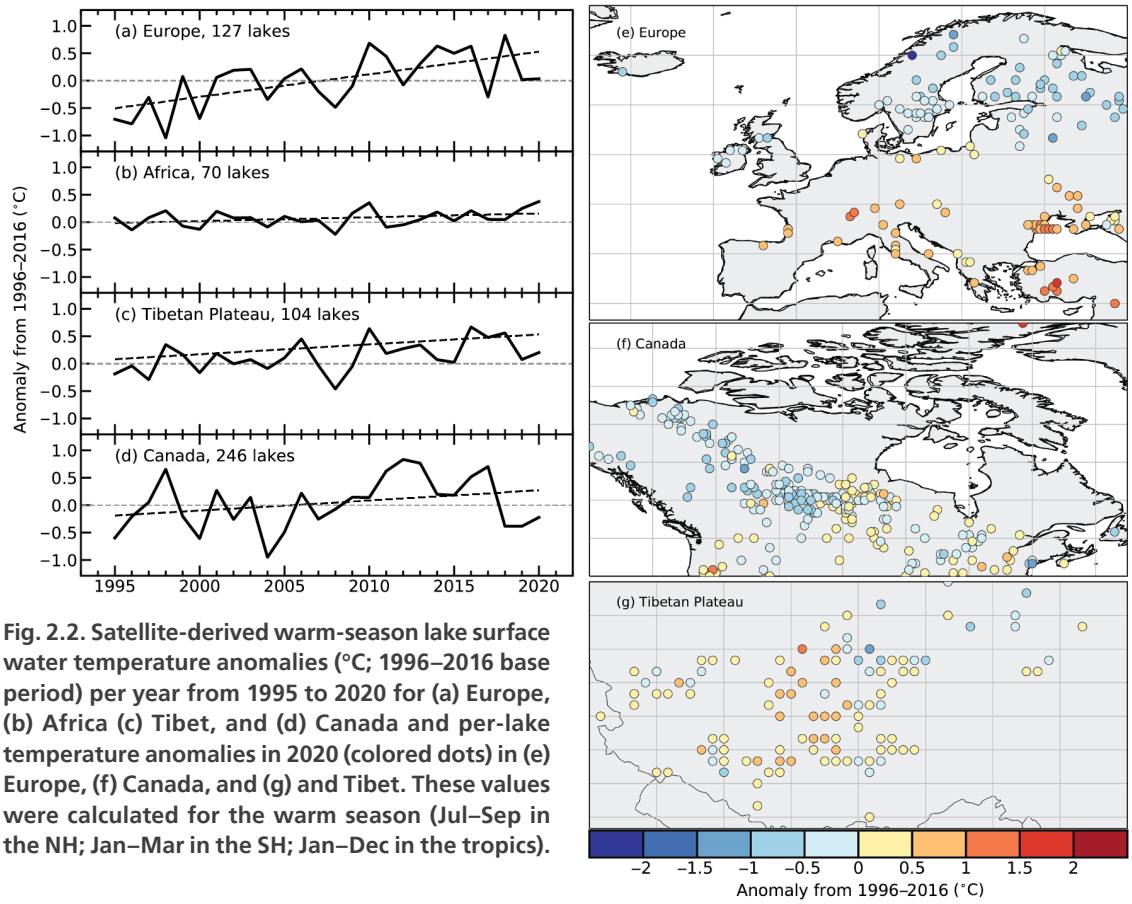

Fig. 2.2. Satellite-derived warm-season lake surface water temperature anomalies (°C; 1996–2016 base period) per year from 1995 to 2020 for (a) Europe, (b) Africa (c) Tibet, and (d) Canada and per-lake temperature anomalies in 2020 (colored dots) in (e) Europe, (f) Canada, and (g) and Tibet. These values were calculated for the warm season (Jul–Sep in the NH; Jan–Mar in the SH; Jan–Dec in the tropics).

Figure 2.3 presents a selection of African lakes (Victoria, Tanganyika, Malawi, Turkana, Rukwa, Albert, Kyoga, Edward, Mweru, Tana, and Bangweulu) for which the LSWT and the LWL normalized anomalies from 1996 to 2020 are reported for each of the lakes, together with the spatial distribution of the 2020 LSWT anomalies. All the lakes exhibit positive LWL anomalies in 2020, while Lakes Turkana, Edward, and Rukwa have notably high LSWT positive anomalies. For these lakes, the LSWT 2020 anomalies were consistently positive across their full spatial extent, while there was a mix of positive and negative anomalies spatially across other lakes. Most of the lakes exhibited an upward long-term trend for both the LSWT and LWL.

The LSWT warm-season averages for midlatitude lakes are computed for summers (July–September in the Northern Hemisphere [NH] and January–March in the Southern Hemisphere [SH]), and whole-year averages (January–December) are presented for tropical lakes (within 23.5° of the equator).

The LSWT time series were derived from satellite observations from the series of Along Track Scanning Radiometers (ATSRs), the Advanced Very High Resolution Radiometers (AVHRRs) on MetOp A and B, and the Sea and Land Surface Temperature Radiometers (SLSTRs) on Sentinel3A and 3B. The retrieval method of MacCallum and Merchant (2012) was applied on image pixels filled with water according to both the inland water dataset of Carrea et al. (2015) and a reflectance-based water detection scheme. The LWL observations for 11 African lakes were analyzed where long time series are available from radar altimetry (Cretaux et al. 2011). The LWL were validated using a set of in situ data over lakes in South America, North America, Russia, and Europe (Ričko et al. 2012). For lakes with sizes comparable to those in East Africa, the accuracy is generally within 0.1 m (Cretaux et al. 2018; Quartly et al. 2020).

The satellite-derived LSWT data are spatial averages for each of 947 lakes, for which high-quality temperature records were available in 2020. The satellite-derived LSWT data were validated with in situ measurements with an average satellite minus in situ temperature difference less than

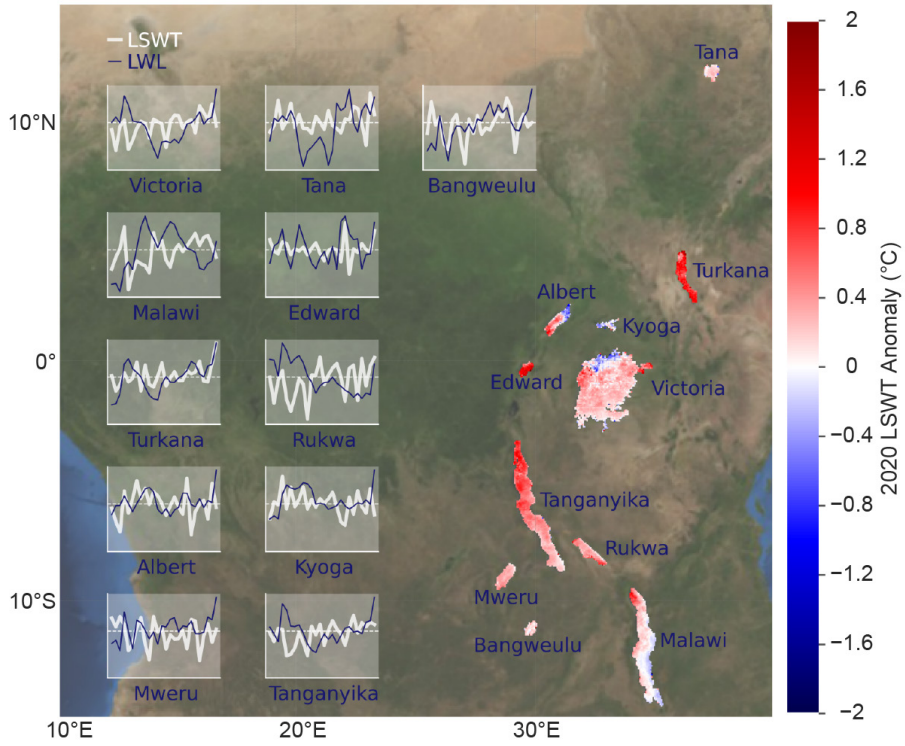

Fig. 2.3. Satellite-derived lake surface water temperature (LSWT) and lake water level (LWL) normalized anomalies relative to the 1996–2016 period from 1995 to 2020 for 11 lakes in East Africa, together with the spatial distribution of the 2020 LSWT anomalies (in °C) for the same lakes.

0.5°C and, consequently, a good agreement was found. Lake-wide average surface temperatures have been shown to provide a more representative picture of LSWT responses to climate change than single-point measurements (Woolway and Merchant 2018).

3) Land and marine temperature extremes—S. E. Perkins-Kirkpatrick, R. J. H. Dunn, R. W. Schlegel, M. G. Donat , and Michael G. Bosilovich.

Averaged over global land regions using the Global Historical Climatology Network-Daily dataset (GHCNDEX; Donat et al. 2013), 2020 recorded the highest number of days where the maximum temperature was above the climatological 90th percentile (TX90p, "warm days"; Fig. 2.4). There were over 70 days, which is almost double the average of 36.5 days during 1961–90, and 10 days more than 2019. The number of cool nights (TN10p, where the minimum temperature was below the 10th percentile) was lower than the 1961–90 average, at just over 20 nights throughout the year. This was below average compared to the last 70 years but comparable to the recent decade.

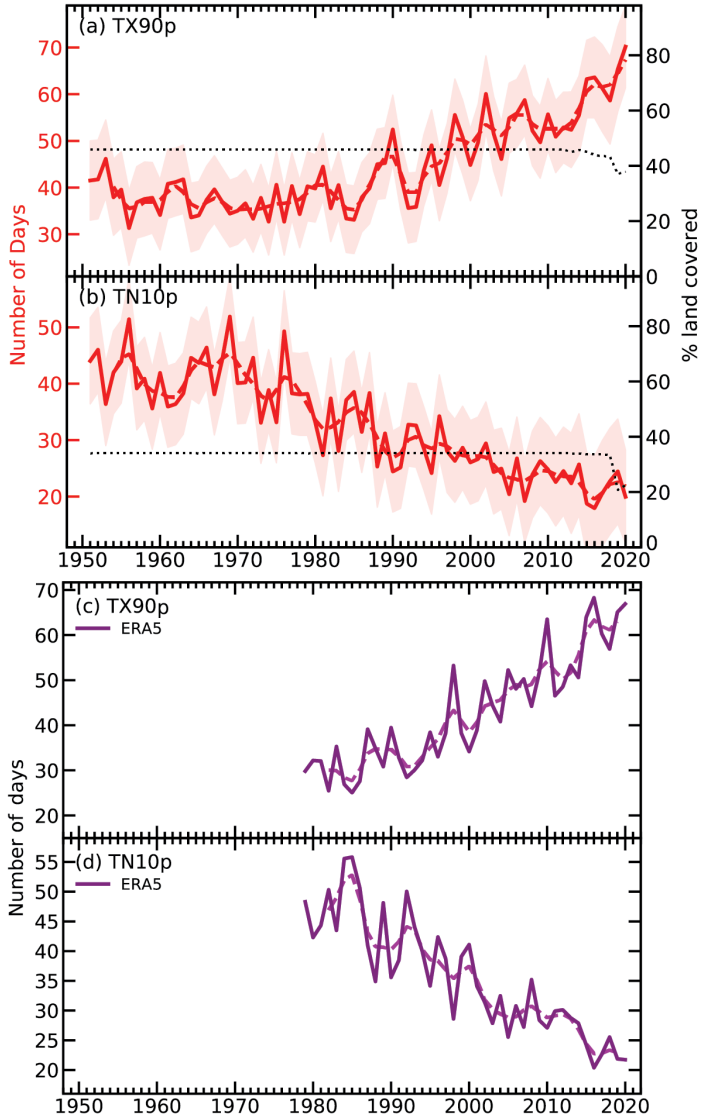

Fig. 2.4. Time series of (a) TX90p (warm days) and (b) TN10p (cool nights) from GHCNDEX relative to 1961–90. The red dashed line shows a binomial smoothed variation and red shading the coverage uncertainties estimated using ERA5 following Brohan et al. (2006). The dotted black line shows the percentage of land grid boxes with valid data in each year. Time series of (c) TX90p (warm days) and (d) TN10p (cool nights) from ERA5 relative to 1981–2010.